Phys Chem Minerals (2004) 31: 306–312
DOI 10.1007/s00269-004-0388-9

ORIGINAL PAPER

A. Yu. Likhacheva · S. A. Veniaminov
E. A. Paukshtis

Thermal decomposition of NH_4-analcime

Received: 11 April 2003 / Accepted: 3 February 2004

Abstract The thermal decomposition of ammonium-exchanged natural analcime is characterized by gas chromatography, IR spectroscopy and X-ray diffraction. The de-ammoniation and dehydroxylation proceed in parallel throughout the decomposition, which evidences the instability of the protonated analcime framework. The mechanism of degassing of NH_4-analcime changes throughout its decomposition. At the initial step, the mechanism of de-ammoniation consists in thermal dissociation of NH_4^+ molecule onto NH_3 and proton (framework OH group) and diffusion of NH_3 out of the structure. Subsequent decomposition and removal of the OH groups lead to a progressive loss of crystallinity. At this step, an apparent activation energy for NH_3 desorption is estimated to be 145($\pm$13) kJ mol^{-1}. This value is within the upper limit of the activation energy characteristic for the NH_3 desorption from proton centres in large-pore zeolites. At the final step, the adsorption of NH_3 and protons onto the defect centres in the amorphosed aluminosilicate framework results in a significant increase of an apparent activation energy for the de-ammoniation and dehydroxylation up to 270($\pm$20) kJ mol^{-1}.

Keywords Ammonium analcime · De-ammoniation · Dehydroxylation · Gas chromatography · IR spectroscopy

A.Yu. Likhacheva (✉)
Institute of Mineralogy and Petrology,
pr.ak.Koptyuga 3, Novosibirsk 90
630090 Russia
Tel:3832 33-24-06
Fax: 3832 33-27-92
e-mail: alih@uiggm.nsc.ru

S. A. Veniaminov · E. A. Paukshtis
Boreskov Institute of Catalysis, pr.ak.Lavrentieva 5,
Novosibirsk 90, 630090 Russia

Introduction

Among the ammonium-bearing minerals, aluminosilicates are the most abundant in the Earth's crust (Loughnan et al. 1983; Compton et al. 1992; Ramseyer et al. 1993; Hall et al. 1994; Harlov et al. 2001). The study of their thermal stability is important for better understanding of the nitrogen evolution in the Earth's crust, in particular, relative to the thermal degassing of ammonium-rich aluminosilicate rocks during metamorphism. Ammonium analcime is a convenient mineral for such a study due to its structural similarity to a wide group of natural ammonium-rich framework aluminosilicates such as the feldspars and feldspathoids (Hori et al. 1986; Yamada et al. 1998; Harlov et al. 2001; Likhacheva et al. 2002; Andrut et al. in press).

Natural analcime ($NaAlSi_2O_6{\cdot}H_2O$) is characterized by a narrow-pore structure (the aperture of inner cavities is within 3 Å) and Al-rich framework (Si/Al $\approx$ 2.2) (Gottardi and Galli 1985). These features appear to make the thermal behaviour of its ammonium form different from that known for the large-pore zeolites (with aperture of inner cavities exceeding 3 Å). Large-pore ammonium zeolites exhibit, as a rule, two main steps during their thermal decomposition: de-ammoniation (decomposition of NH_4^+ to $NH_3 + H^+$ and removal of NH_3, leaving proton adhered to the framework O as OH group) and dehydroxylation (removal of the framework OH groups). These two steps are well separated, as is seen from the thermogravimetric curves containing two peaks at 250–450 and 500–700 °C (Weeks et al. 1975; Beyer et al.1977). In this case, what is important is the formation of a chemically active H form after the removal of NH_3. For Al-rich zeolites with Si/Al <2, it has been shown experimentally (Kuhl and Schweizer 1975; Barthomeuf 1987) and by quantum-chemical calculations (Pelmenschikov et al. 1992) that the protonated framework (H form) is unstable such that the removal of NH_3 from the structure leads to amorphization.

In analcime, the NH_4^+ molecules (R = 1.42 Å) occupy one type of position (W site) in the framework cavities (Moroz et al. 1998; Yamada et al. 1998). The DTG curve indicates only one peak corresponding to the 12.2% weight loss between 400 and 700 °C which is a result of both de-ammoniation and dehydroxylation (Likhacheva and Paukshtis 2000). This is similar to the DTG curves for the natural ammonium feldspar buddingtonite ($NH_4AlSi_3O_8$) and natural ammonioleucite ($NH_4AlSi_2O_6$), which show one main step with respect to weight loss (Voncken et al. 1988; Hori et al. 1986). This means that the de-ammoniation and dehydrohylation steps are hardly separated during the thermal decomposition of these three minerals. However, a detailed investigation of the extent to which these two steps overlap has not been made. In our opinion, this question is of interest with respect to (1) the existence of the protonated forms of natural rock-forming aluminosilicates and (2) the mechanism for degassing of natural ammonium-rich aluminisilicates.

For the NH_4-analcime, the degree of amorphization is proportional to the extent of the weight loss. The detailed structural analysis of partially de-ammoniated NH_4-analcime has revealed the appearance of an additional pseudocubic phase, which is supposed to be H-analcime (Miroshnichenko et al. 2002). This phase is characterized by broad X-ray peaks, which diminish in intensity along with the removal of NH_3, and disappear after the 12.2% weight loss. The nature of proton centres formed at de-ammoniation is unclear.

To characterize in more detail the mechanism of thermal decomposition of NH_4-analcime we present here the results of gas chromatography and thermogravimetry, as well as IR spectroscopy combined with X-ray powder diffraction (XRD) data. On this basis, the mechanism of NH_3 removal as well as the nature of the proton centres (OH groups) produced at different stages of de-ammoniation of the NH_4-analcime are discussed.

Experimental

Material

The starting material was a well-crystallized natural analcime $Na_{0.94}Al_{0.94}Si_{2.06}O_6 \cdot H_2O$ (by X-ray fluorescence) from veins in a basalt (Nidym river, Siberian platform). The crystals were crushed and the fraction 0.2–0.4 mm was doubly exchanged with an NH_4NO_3- saturated solution at 140 °C during 3 days. The details of the exchange procedure are reported in Likhacheva et al. (2002). According to flame photometry data, the degree of exchange achieved was greater than 97%. This allows the composition of the final material to be approximated as $(NH_4)_{0.94}Al_{0.94}Si_{2.06}O_6$.

Both the initial and NH_4-exchanged analcimes were also characterized by X-ray diffraction (XRD). The XRD analysis has confirmed the transition from the orthorombic (pseudocubic) unit cell (a = 13.729, b = 13.686, c = 13.710 Å) in the natural analcime to the tetragonal unit cell (a = 13.218, c = 13.710 Å) in the NH_4-analcime consistent with the observations of Moroz et al. 1998.

X-ray analysis

X-ray powder diffraction analysis was used to check the phase content of the exchanged material, as well as to determine the unit-cell parameters of the initial and ammonium-exchanged analcime and the intensity of the X-ray peaks of the calcined NH_4-analcime. XRD patterns were recorded using a powder diffractometer DRON-3 with monochromatized $Cu_{K\alpha}$ radiation. The unit-cell parameters were refined by the least-squares method from the XRD spectra recorded with corundum as an internal standard.

Thermal analysis

The thermogravimetry (TG) analysis was performed on a Mettler TA-3000 thermobalance with a heating rate of 3 °C min^{-1} at 25–770 °C in air, and the sample weight of 30 mg.

Gas chromatography

The quantitative determination of NH_3 and H_2O removed from the NH_4-analcime during its thermal decomposition was carried out by gas chromatographic analysis on a device described in Veniaminov and Barannik (1980). This device is composed of a quartz microreactor connected to a series-produced chromatograph containing two thermal conductivity detectors. The signals from the thermocouple embedded in the zeolite and those from the detectors are sent to a multichannel converter. The data were collected, stored and processed using the MULTICHROM program. A Chromosorb-104 column was used for the separation of NH_3 and H_2O at 130 °C. Calibration for NH_3 was accomplished using a dosed reference mixture of NH_3 and He. Calibration for H_2O was done using a dosed probe of He saturated with water vapour under a fixed ambient temperature. The experimental detection limit for NH_3 and H_2O was determined to be 10^{-4} mg. Several test analyses were made for the measurement of N_2 at different stages during thermal degassing of the NH_4-analcime. The nitrogen concentration did not exceed the background limit.

Before the measurement, the sample (20 mg, 0.2–0.4-mm fraction) was kept in a flow of dry He at 100 °C until the physically adsorbed water was removed. The sample was then heated with a dry He flow rate of 40 $mlmin^{-1}$ at a rate 3 °C min^{-1} up to 756 °C, and then held at 756 °C to the end of degassing. The time for the probe collection and analysis was 5 min. The evaluation of around 70 analyses accumulated during the measurement produced the time/temperature dependence for NH_3 and H_2O concentration in the gas flow. On this basis, the temperature dependence for the rate of NH_3 and H_2O removal was derived, which makes it possible to compare the gas chromatography and thermogravimetry data.

IR spectroscopy

IR measurements were conducted for a sample of NH_4-analcime cyclically heated in the spectrometer cell to follow the changes in the N–H and O–H vibrations in 1200–4000 cm^{-1} region during de-ammoniation and dehydroxylation. IR spectra were recorded using a FTIR-8300 spectrophotometer (Shimazu) with resolution 1 cm^{-1} at room temperature for 10 min at each temperature step between 300 and 700 °C on self-supported pellets in the evacuated cell. The heating rate was 10 ° C min^{-1}. The band positions and integral intensities of the individual IR bands were determined using the Origin 5.1 program. To compare the IR data with the sample crystallinity, another portion of the NH_4-analcime powder was cyclically heated in an evacuated quartz tube under the same conditions (vacuum, fraction size, heating regime) as for IR measurements, with registration of XRD spectra at each temperature step.

Results and discussion

Gas chromatography

The temperature dependence for the rate of NH_3 and H_2O removal is presented in Fig. 1 together with the thermoanalytical DTG curve for the NH_4-analcime. According to the gas chromatography data, the total NH_3 loss is 8.09 wt% and the total H_2O loss is 5.1 wt%. These quantities are in satisfactory agreement with the total weight loss of 12.664 wt% determined by thermogravimetric measurements. It should be mentioned that the total weight loss obtained by our TG analysis is about 0.46 wt% above the value obtained previously due to a higher upper temperature limit for the analysis.

As it is seen from Fig. 1, the total ($NH_3 + H_2O$) gas chromatography curve approximates well the DTG curve, with the exception of a small peak indicating a 1.5 wt% water loss at 200–400 °C. This quantity is below the detection limit of the IR analysis. Thermogravimetric measurements show a loss of 0.69 wt% over this temperature interval. The presence of H_2O may partially be attributed to the dehydration of the non-exchanged phase (not registered by XRD). According to the structural data of Yamada et al. (1998), the NH_4-analcime is a nominally dry phase, as the NH_4^+ molecules occupy the H_2O positions. This is in accordance with our IR data showing no appreciable bands in the region of H_2O vibrations (Likhacheva et al. 2002). However, a small quantity of H_2O (0.5–1%) has also been registered in both synthetic NH_4-analcime and natural ammonioleucite, these two minerals being structural and chemical analogues (Barrer et al. 1953; Hori et al. 1986). According to the broad peak at 200–400 °C (Fig. 1), a disordered distribution throughout the NH_4-analcime structure is supposed for this small quantity of H_2O.

Figure 1 shows that de-ammoniation and dehydroxylation proceed in parallel, except for the initial step when about 0.28 wt% of NH_3 is lost before the dehydroxylation starts. The change in the molar ratio NH_3/H_2O during thermal degassing of the NH_4-analcime is shown in Fig. 2. This ratio must equal 2, provided that, for two NH_3 molecules, one H_2O molecule is formed and immediately removed, in accordance with the decomposition scheme outlined above:

$$2NH_4\text{-}Z \rightarrow 2H\text{-}Z + 2NH_3 \rightarrow Z + H_2O$$

(Z = zeolite aluminosilicate framework). Figure 2 shows that the ratio NH_3/H_2O is appreciably higher than 2 over almost the whole process of degassing. The H_2O fraction increases only at the final stage of de-ammoniation. This means that, even if de-ammoniation and dehydroxylation are parallel on the overall process scale, there is a small but distinct gap between these two steps of thermal evolution of the NH_4-analcime.

The course of thermal degassing of NH_4-analcime is next described using the temperature dependence of the rate constant of de-ammoniation (dehydroxylation) $\log K = f(T^{-1})$. The rate constant was calculated assuming a first-order relationship for the de-ammoniation (dehydroxylation) rate with respect to the NH_3 (H_2O) concentration in the sample: $\kappa = W_t/A_t$, where W_t is the rate of NH_3 (H_2O) removal from the sample taken from the gas chromatography curves in Fig. 1. A_t represents the current concentration of NH_3 (H_2O) in the sample derived from the gas chromatography data (not presented here).

The $\log K = f(T^{-1})$ curves for NH_3 and H_2O are shown in Fig. 3. The observed bend of these curves indicates

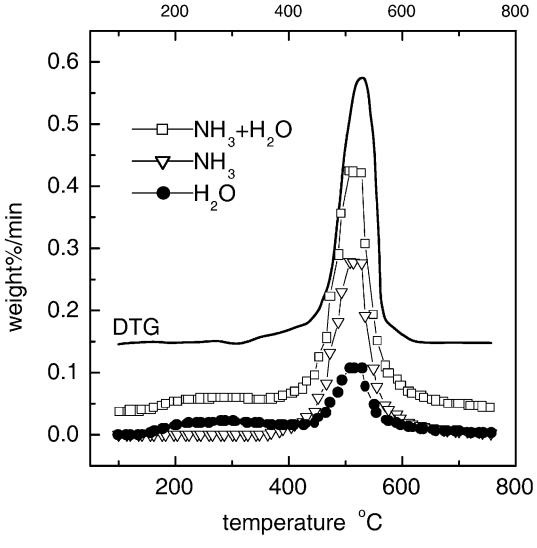

Fig. 1 Temperature dependence for the rate of NH_3, H_2O and $NH_3 + H_2O$ removal during linear heating of NH_4-analcime, derived from the gas chromatography data, and the DTG curve of NH_4-analcime obtained by thermogravimetry. The ($NH_3 + H_2O$) and DTG curves are shifted along the *y* axis. Heating rate: 3 °C min^{-1}

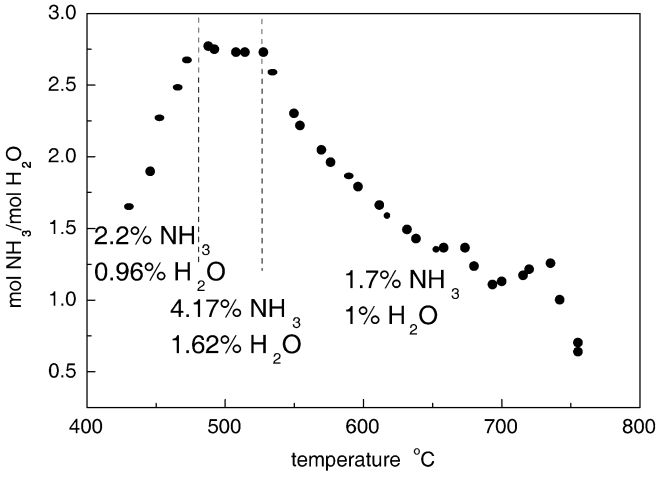

Fig. 2 Molar ratio NH_3/H_2O in the gas mixture removed during thermal decomposition of NH_4-analcime, obtained by gas chromatography. The total loss of NH_3 and H_2O at the different steps of decomposition (separated by *vertical dashed lines*) is indicated

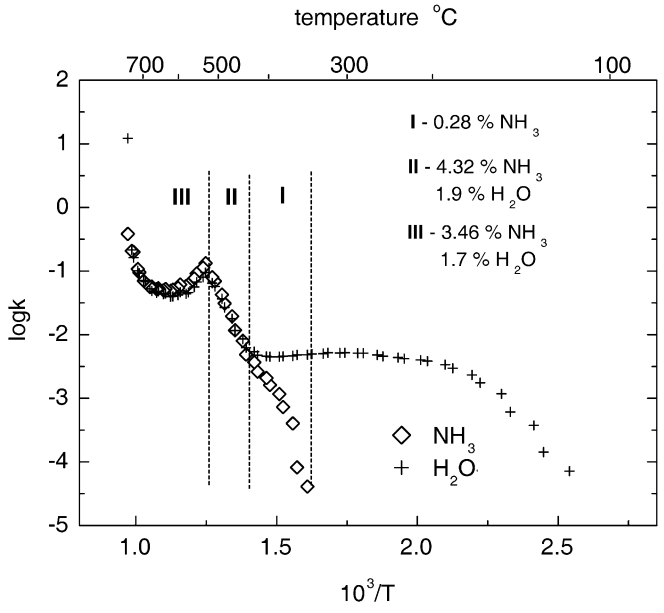

Fig. 3 Temperature dependence of the first-order rate constant for desorption of NH_3 and H_2O during linear heating of NH_4-analcime. The total loss of NH_3 and H_2O at the different steps of decomposition (separated by *vertical dashed lines*) is indicated

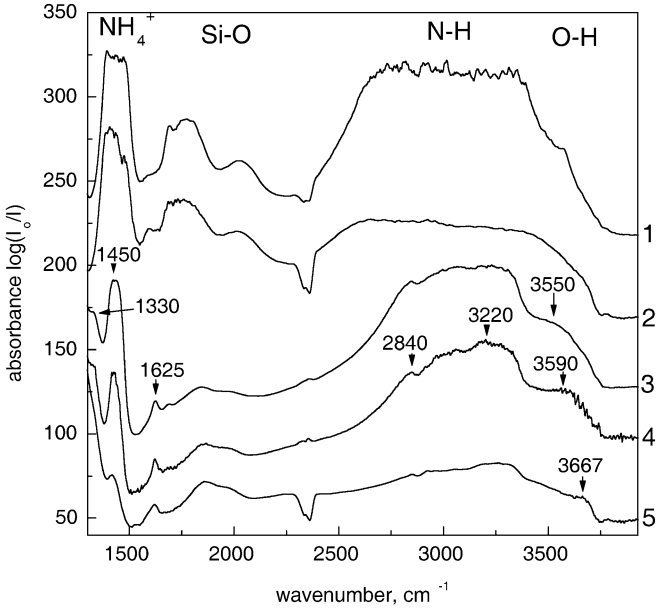

Fig. 4 IR spectra of NH_4-analcime after vacuum treatment at 300 °C (*1*), 400 °C (*2*), 550 °C (*3*), 600 °C (*4*), and 700 °C (*5*)

that the mechanism of degassing of NH_4-analcime changes throughout the course of its thermal decomposition. The sharp bend of the H_2O curve at $x = 1.4$ ($10^3/K^{-1}$) corresponds to the beginning of dehydroxylation. The linear part of the NH_3 and H_2O curves (marked as I and II on Fig. 3) corresponds to the first half of the weight loss during de-ammoniation and dehydroxylation. The linearity of these curves implies a first-order relationship for the removal of NH_3 and H_2O from the sample. A first-order relationship is typical for the rate of the NH_3 desorption from the acid proton centres in large-pore zeolites (Post and van Hooff 1984; Karge and Dondur 1990). As has been mentioned, the overall crystallinity of large-pore zeolites is preserved during the NH_3 desorption. By analogy, it may be assumed that the mechanism of NH_3 removal from the NH_4-analcime on the linear part of the curve consists of the thermal dissociation of the NH_4^+ molecule into NH_3 and proton (framework OHgroup), and diffusion of NH_3 out of the structure. It should be noted that the activation energies for de-ammoniation and dehydroxylation must have relatively close values because the corresponding curves coincide.

Further decomposition of the NH_4-analcime proceeds in a non-linear manner (part III: in Fig. 3), which implies a deviation from the first-order relationship between the rate of the NH_3 (H_2O) removal and the concentration of these substances in the sample. The reasons for this deviation are not definitely clear. To our opinion, the achievement of some "critical" degree of amorphization during the dehydroxylation may be regarded as the most probable reason for the observed non-linearity. This assumption is supported by the XRD and IR data (described below) showing a sharp amorphization and collapse of structure channels after the removal of about 60% of the total ammonium content. This amount roughly corresponds to the quantity of NH_3 measured at the linear (I–II) part of the NH_3 curve in Fig. 3.

The complexity of the non-linear part and, in particular, some straightening of the NH_3 and H_2O curves in the closing stage of degassing, suggest that the character of reaction, leading to the removal of these substances from analcime, differs from that corresponding to the linear part of the curves. Most probably this is due to defects accumulated in the amorphosed framework, after the dehydroxylation has reached its half-way point. In the linear part of the NH_3 curve, an apparent activation energy of 145 (± 13) kJ $mol^{-1}$is estimated. For comparison, the apparent activation energy for NH_3 desorption from the acidic proton centres in large-pore zeolites lies between 80 and 150 kJ mol^{-1} (Shannon et al. 1985; Karge and Dondur 1990; Yin et al. 1997). In the steep part of the NH_3 and H_2O curves [at $x = 1.0$ $(10^3K)^{-1}$, Fig. 3], corresponding to the final stage of degassing, an apparent activation energy of 270(± 20) kJ mol^{-1} is estimated. This means that the last portion of NH_3 and H_2O (about 1% of the initial content) is much more strongly held in the amorphosed aluminosilicate, as compared to the initial step of degassing.

IR spectroscopy

IR spectra for NH_4-analcime registered at different temperature steps are displayed in the region of N–H and O–H vibrations in Fig. 4. In the region of 1250–4000 cm^{-1} the IR spectrum for NH_4-analcime contains

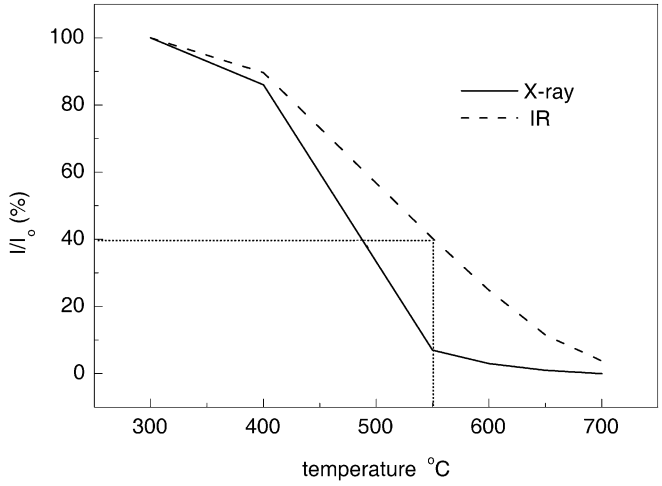

Fig. 5 Relative intensities of the ammonium IR band at 1450 cm^{-1} and the (121) X-ray peak of NH_4-analcime, after stepwise vacuum heating. *Dotted line* marks the transition to a collapsed structure after removal of about 60% of ammonium, according to the intensity of the IR band at 1450 cm^{-1}

intensive bands of bending (1450 cm^{-1}), overtones (2500–3000 cm^{-1}) and stretching vibrations (3000–3400 cm^{-1}) for the NH_4^+ molecule (Likhacheva et al. 2002). In the region of 1700–2200 cm^{-1}, overtone framework Si–O bands are observed. The IR spectrum recorded at 300 °C may be regarded as close to that recorded at room temperature since no appreciable changes are observed by gas chromatography and XRD analysis at this temperature.

The starting of de-ammoniation at 400 °C is reflected by a slight decrease of the ammonium bands at 1450 and 2500–3400 cm^{-1}. This is also accompanied by a decrease in the XRD peaks (Fig. 5), which is in agreement with the data of Miroshnichenko et al. 2002. A weak shoulder is observed in the region of the O–H vibrations at 3500–3600 cm^{-1}. The form of this shoulder would suggest both a disordered distribution and small concentration of the OH groups in the structure. The extent of de-ammoniation estimated from the intensity of the ammonium IR band roughly corresponds to the linear part of the NH_3 removal revealed by gas chromatography (Fig. 3, part I-II). Therefore, the shoulder observed at 3500–3600 cm^{-1} corresponds to the framework OH groups formed at the first stage of de-ammoniation. In accordance with the gas chromatography data, these groups are unstable and disappear right after they are formed, which results in a negligible intensity for the corresponding IR band.

A progressive de-ammoniation is seen from an appreciable decrease of the ammonium bands at 550 °C. The Si–O overtone spectrum changes sharply due to almost complete amorphization, which is confirmed by XRD (Fig. 5). As is seen from Fig. 5, a high degree of amorphization is achieved when approximately 60% of ammonium is lost. The narrowing of the ammonium band at 1450 cm^{-1} may serve as an additional evidence for the amorphization and collapse of the framework cavities hosting NH_4^+ molecules. This results in a disarrangement of the hydrogen bonding between the NH_4^+ molecule and the framework and, as a consequence, leads to the degeneration of bending mode at 1450 cm^{-1}. Simultaneously, the shoulder of the O–H vibrations becomes more prominent due to the accumulation of hydroxyl groups in the sample. The frequency value and a large half-width (about 250 cm^{-1}) of this band are typical of OH groups associated with the non-framework Al species (Shannon et al. 1985). The term non-framework is generally applied to Al atoms having one or more Al–O framework bonds broken as a result of dehydroxylation (Freude et al. 1983; Corma 1995; Alvarez et al. 1997). The process leading to the formation of the non-framework Al is called de-alumination (Shannon et al. 1985; Bodart et al. 1986). For Al-rich framework aluminosilicates, like analcime, de-alumination is an essential part of the amorphization process. Thus the appearance of OH groups associated with non-framework Al is consistent with an essentially amorphous state for the sample. The high-frequency shift of this shoulder observed at higher temperatures is known to associate with a progressive de-alumination of the framework lattice (Shannon et al. 1985).

Therefore the character of the hydroxyl groups changes at different steps of de-ammoniation of the NH_4-analcime. The framework OH groups formed during an early stage of de-ammoniation are unstable, which results in dehydroxylation, leading to the breakdown of Si,Al–O framework bonds and amorphization. Further de-ammoniation results in the formation of OH-groups associated with the non-framework Al species, generally designated as hydroxyaluminum complexes (Shannnon et al. 1985; Pelmenschikov et al. 1992), located in the amorphosed areas of the crystal lattice. According to the extent of de-ammoniation reached at 500 °C, the formation of these OH groups proceeds in the non-linear part of the thermal degassing of the NH_4-analcime (part III in Fig. 3).

At 550 °C two additional bands at 1330 and 1625 cm^{-1} appear in the IR spectrum of NH_4-analcime. These bands are typical of NH_3 bonded to Lewis acid sites (marked as ≡ Al:NH_3), the latter representing a coordinated unsaturated Al species (Corma 1995). These sites are widely observed in the large-pore zeolites in association with de-aluminated parts of the framework (Corma 1995; Yin et al. 1997). The IR band resulting from the bending motion of the NH_3 molecule is generally observable between 1300 and 1340 cm^{-1} (as in this case) when sufficient quantities of non-framework Al is present (Yin et al. 1997). The extinction coefficient for the ≡ Al:NH_3 band at 1625 cm^{-1} is known to be less than that for the NH_4^+ ion band at 1450 cm^{-1} by an order of magnitude (Yin et al. 1997). This means that the amount of NH_3 molecules bonded to Lewis sites is comparable to that of the residual NH_4^+ molecules. Note that the 1625 cm^{-1} band remains stable whereas the ammonium band at 1450 cm^{-1} diminishes at higher temperatures. It

follows that the adsorption of NH_3 on Lewis sites represents the intermediate step for NH_3 removal at the final stage of de-ammoniation of NH_4-analcime. The Lewis sites are known to easily adsorb NH_3 molecules to form stable complexes (Corma 1995). The adsorption of NH_3 onto the Lewis sites is probably facilitated by a high degree of disarrangement in the structure, thus preventing fast diffusion of NH_3 through the sample.

These observations indicate that there are at least two types of defect centres associated with a de-aluminated (amorphosed) part of the analcime framework that adsorb NH_3 molecules (Lewis sites) and protons (hydroxyaluminum complexes) after the dissociation of the NH_4^+ molecules at the progressive stage of de-ammoniation. These centres are most probably the major factors that inhibit the NH_3 and H_2O removal in the final stage of degassing. The chemical character of bonding in the $\equiv$ Al:NH_3 complexes and the non-framework Al-OH complexes makes them more stable as compared to the H-bonded NH_4^+ molecules and the framework OH groups. The fraction of NH_3 adsorbed on Lewis sites remains almost constant up to 700 °C. The fraction of the OH groups diminishes at high temperature, but is still present at 700 °C. Therefore the thermal decomposition of the NH_4-analcime is not fully complete over the temperature range used during IR measurements. This is consistent with our gas chromatography data.

Conclusions

The de-ammoniation and dehydroxylation proceed in parallel over the thermal decomposition of the NH_4-analcime. This evidences the instability of the protonated analcime framework formed after the removal of NH_3, and leads to a negligibly small concentration of OH groups formed at the initial step of de-ammoniation.

The mechanism of de-ammoniation and dehydroxylation changes throughout the thermal decomposition of NH_4-analcime. In the initial step, the mechanism for NH_3 removal consists in thermal dissociation of NH_4^+ molecules onto NH_3 and a proton (framework OH group) as well as diffusion of NH_3 out of the structure. An apparent activation energy for NH_3 desorption is estimated to be 145($\pm$ 13) kJ mol^{-1}. Subsequent decomposition and removal of the OH groups (dehydroxylation) lead to a progressive loss of crystallinity. This step accounts for about 60% of the total weight loss. Then, a collapse of the structure occurs.

In the final step, the adsorption of NH_3 and protons onto the defect centres accumulated in the amorphosed framework hinders the de-ammoniation and dehydroxylation. The chemical character of bonding in the $\equiv$ Al:NH_3 complexes and the non-framework Al–OH complexes makes them more stable as compared to the H-bonded NH_4^+ ions and the framework OH groups. This causes an appreciable increase in the activation energy for NH_3 and H_2O desorption to 270($\pm$ 20) kJ mol^{-1}. This may favour the conservation of a small part of nitrogen as the $\equiv$ Al:NH_3 complex in the amorphosed aluminosilicate up to relatively high temperatures, as regards the conditions of thermal degassing of the natural ammonium-rich aluminosilicates.

Acknowledgements We are grateful to Dr. D.Harlov and Dr. M.Mookherjee for the review of the manuscript, as well as to Dr. G.P.Valueva and Dr. N.K.Moroz for their helpful comments. This work is supported by RFBR grant no.02–05–65313, 04-05-64351.

References

Alvarez LJ, Ramirez-Solis A, Giral PB (1997) Mechanisms of formation of extraframework Al_2O_3 in zeolites. Zeolites 18: 54–62

Andrut M, Harlov DE, Najorka J Characterisation of ammonioleucite $(NH_4)[AlSi_2O_6]$ and ND_4-ammonioleucite $(ND_4)[AlSi_2O_6]$ using IR spectroscopy and Rietveld refinement of XRD spectra. Mineral Mag (in press)

Barrer RM, Bayhnam JW, McCallum N (1953) Hydrothermal chemistry of silicates. Part V. Compounds structurally related to analcite. J Chem Soc 4035–4041

Barthomeuf D (1987) Zeolite acidity dependence on structure and chemical environment. Mat Chem Phys 17: 49–71

Beyer HK, Jacobs PA, Uytterhoeven JB, Till F (1977) Thermal stability of NH_4-chabazite. JCS Faraday Trans1 73: 1111–1118

Bodart P, Nagy JB, Debras G, Gabelica Z, Jacobs PA (1986) Aluminum siting in mordenite and dealumination mechanism. J Phys Chem 90: 5183–5190

Compton JS, Willams LB, Ferrell RE Jr (1992) Mineralization of organogenic ammonium in the Monterey Formation, Santa Maria and San Joaquin Basins, California, USA. Geochim Cosmochim Acta 56: 1979–1991

Corma A (1995) Inorganic solid acids and their use in acid-catalyzed hydrocarbon reactions. Chem Rev 95: 559–614

Freude D, Frochlich T, Pfeifer H, Sheler G (1983) NMR studies of alumimium in zeolites. Zeolites 3: 171–177

Gottardi G, Galli E (1985) Natural zeolites. Springer Berlin Heidelberg NewYork, pp 9–13

Hall A, Stamatakis MG, Walsh JN (1994) Ammonium enrichment associated with diagenetic alteration in Tertiary pyroclastic rocks from Greece. Chem Geol 118: 173–183

Harlov DE, Andrut M, Poter B (2001) Characterisation of buddingtonite $(NH_4)[AlSi_3O_8]$ and ND_4-buddingtonite $(ND_4)[AlSi_3O_8]$ using IR spectroscopy and Rietveld refinement of XRD spectra. Phys Chem Miner 28: 188–198

Hori H, Nagashima K, Yamada M, Miyawaki R, Marubashi T (1986) Ammonioleucite, a new mineral from Tatarazawa, Fujioka, Japan. Am Mineral 71: 1022–1027

Karge HG, Dondur V (1990) Investigation of the distribution of acidity in zeolites by temperature-programmed desorption of probe molecules. 1. Dealuminated mordenites. J Phys Chem 94: 765–772

Kuhl GH, Schweizer AE (1975) Structural stability of sodium ammonium zeolite X. J Catal 38: 469–476

Likhacheva A, Paukshtis E (2000) IR spectroscopy of thermal decomposition of ammonium analcime. J Conf Abstr EMPG VIII, Bergamo,Italy,16–19 April 2000, p.64

Likhacheva AYu, Paukshtis EA, Seryotkin YuV, Shulgenko SG (2002) IR spectroscopic characterization of NH_4-analcime. Phys Chem Miner 29: 617–623

Loughnan FC, Roberts FI, Lindner AW (1983) Buddingtonite (NH_4-fieldspar) in Condor oilshale deposit, Quinland, Australia. Miner Mag 47(3): 323–334

Miroshnichenko YuM, Drebushchak VA, Seryotkin YuV (2002) Detection of the H-form of analcime. J Conf Abstr Zeolite'02,Thessaloniki, Greece, 2002, p.235

Moroz NK, Seryotkin YuV, Afanassiev IS, Belitsky IA (1998) Arrangement of the extraframework cations in NH_4-analcime. J Struct Chem Engl Tr 39 (2): 281–283

Pelmenschikov AG, Paukshtis EA, Edisherashvili MO, Zhidomirov GM (1992) On the Loewenstein rule and mechanism of zeolite dealumination. J Phys Chem 96: 7051–7055

Post JG, van Hooff JHC (1984) Acidity and activity of H-ZSM-5 measured with NH_3- t.p.d. and *n*-hexane cracking. Zeolites 4: 9–14

Ramseyer K, Diamond LW, Boles JR (1993) Authigenic K-NH4-feldspar in sandstones: a fingerprint of the diagenesis of organic matter. J Sedimental Petrol 63(6): 1092–1099

Shannon RD, Gardner KH, Staley RN, Bergeret G, Gallezot P, Auroux A (1985) The nature of the nonframework aluminum species formed during the dehydroxylation of H–Y. J Phys Chem 89: 4778–4788

Veniaminov SA, Barannik GB (1980) Intermediates in the interaction of 1-butene and butadiene with an iron-antimony oxide catalyst. React Kinet Catal Lett 13(4): 413–418

Vonken JHL, Konings RJM, Jansen JBH, Woensdregt CF (1988) Hydrothermally grown buddingtonite, an anhydrous ammonium feldspar ($NH_4AlSi_3O_8$). Phys Chem Miner 15: 323–328

Weeks TJ, Angell CL, Bolton AP (1975) The thermochemical properties of ammonium exchanged erionite. J Catal 38: 461–468

Yamada M, Miyawaki R, Nakai I, Izumi F, Nagashima K (1998) A Rietveld analysis of the crystal structure of ammonioleucite. Mineral J 20(3): 105–112

Yin F, Blumenfeld AL, Gruver V, Fripiat JJ (1997) NH_3 as probe molecule for NMR and IR study of zeolite catalyst acidity. J Phys Chem 101: 1824–1830